EXPERIMENTAL HEAT TRANSFER TO BLUNT AXISYMMETRIC BODIES NEAR THE LIMIT OF CONTINUUM FLOW

By

J. Leith Potter and John T. Miller

von Kármán Gas Dynamics Facility

ARO, Inc.

a subsidiary of Sverdrup and Parcel, Inc.

August 1962

ARO Project No. 306159

ABSTRACT

This is a report of measurements of average heat-transfer rates to blunt-nosed, axisymmetric, cold-walled bodies in a low-density, hypervelocity wind tunnel. Stream density was such that Reynolds and Knudsen numbers, based on nose radius and conditions immediately behind the bow shock, varied from 5 to 20 and 0.11 to 0.056, respectively. Thus, scaling on the basis of Knudsen number, these conditions may be said to simulate a body of one-foot nose radius at as much as 315,500-ft altitude.

Heat-transfer rates are discussed in relation to the flow model successfully used in the past for studies of flows of high Reynolds number. In this context, it was found that measured heat-transfer rates to hemispheres below shock-layer Reynolds numbers of 20 exhibited a decreasing nondimensionalized rate relative to that estimated by methods appropriate to high Reynolds number conditions. This behavior is in accord with various applicable theories. On the other hand, rates for the flat-faced bodies showed no tendency to decrease in the range of conditions investigated, and they were somewhat higher than predicted by theories for high Reynolds numbers.

CONTENTS

TABLES

ILLUSTRATIONS

Figure

NOMENCLATURE

d	Shock thickness (see Fig. 1)
H_o	Total enthalpy, e.g., Btu/lb
H_w	Enthalpy corresponding to body surface conditions
M_∞	Free-stream Mach number
Pr	Prandtl number
$\dot{q}$	Local heat-transfer rate, e.g., Btu/sec ft^2
$\dot{q}_{avg}$	$\frac{1}{\text{Area}} \int_{\text{Area}} \dot{q}\, d\,\text{Area}$
$\dot{q}_{avg\ fm}$	$\frac{1}{\text{Area}} \int_{\text{Area}} \dot{q}_{fm}\, d\,\text{Area}$
$\dot{q}_{fm}$	Free-molecular flow heat-transfer rate for complete accommodation; $(\rho_\infty/2)\, U_\infty^3 \cos\theta$ herein
$\dot{q}_o$	Heat-transfer rate at stagnation point
$\dot{q}_{o\ fm}$	Free-molecular flow heat-transfer rate at stagnation point
R	Radius of body (see Fig. 1)
Re_2	Reynolds number downstream of bow shock* = $R\ \rho_\infty\ U_\infty/\mu_2$
Re_∞	Reynolds number based on free-stream conditions = $R\ \rho_\infty\ U_\infty/\mu_\infty$
$(dU_e/ds)_o$	Gradient of velocity at edge of boundary layer at stagnation point
U_∞	Free-stream velocity
γ	Ratio of specific heats of the gas
Λ	Thickness of shock layer (see Fig. 1)
θ	Angular coordinate (see Fig. 1)
λ_2	Mean free path immediately downstream of bow shock*
μ_2	Viscosity of gas immediately downstream of bow shock*
μ_∞	Viscosity of gas in free stream
ρ_2	Mass density immediately downstream of bow shock*
ρ_∞	Mass density of gas in free stream

*For purposes of defining these quantities, the bow shock is assumed thin and separated from the boundary layer.

1.0 INTRODUCTION

The heat transfer encountered by bodies at high altitudes and high velocities is a subject of current interest to both practical designers and theoreticians. Although the altitudes where maximum re-entry heating rates occur often are low enough that the effects considered here are insignificant, a knowledge of heat transfer at higher altitudes is necessary for the design of many vehicles that will enter the atmosphere after orbiting or interplanetary flight. The subject is also of considerable theoretical interest because of the combined influences of such phenomena as vorticity, slip, temperature jump, and non-negligible ratios of boundary-layer thickness to body radius. These phenomena are poorly understood, and available theoretical estimates of their effects on heat transfer differ significantly.

Blunt-faced body shapes are of most practical interest because of well-known aerodynamic heating problems. The hemisphere and the flat-faced shape were chosed for the investigation reported herein. The hemisphere has been studied most intensively, and there is qualitative agreement between theory and experiment; i. e., passing from the high Reynolds number regime to very low Reynolds numbers results in an initial increase in heat transfer to the body, followed by a decrease relative to that expected on the basis of methods devised for the high Reynolds number or "thin boundary-layer" case. This decrease in relative heating rate with increasing rarefaction continues as the free-molecule rate is asympotically approached. Such complete theoretical study has not been devoted to the flat nose, but it was thought that the above described behavior would be delayed to lower Reynolds numbers for this shape. Thus, the latter would serve as a "control" shape.

Based on the delineation of the flow regimes proposed by Probstein (Ref. 1) it may be said that extensive data have been obtained for the "boundary-layer" regime, and some data have been published for the "vorticity-interaction" and "viscous-layer" regimes. This is a report of initial results of a new experimental investigation. The data presented here extend the measurements of heat transfer into the "incipient merged-layer" and the "fully merged-layer" regimes which cover the altitude range from about 55 to 60 miles for a characteristic body dimension of one foot. These correlations of tunnel conditions and altitude regimes are based on a comparison of mean free path calculations; that is, the ratio of

---

Manuscript released by authors July 1962.

mean free path behind the normal shock to the model nose radius was taken to correspond with the same ratio based on a full-scale body dimension of one foot in free flight.

2.0 WIND TUNNEL

The low-density, hypervelocity, continuous flow, wind tunnel, referred to as the LDH Tunnel, in operation at the von Kármán Gas Dynamics Facility of the Arnold Engineering Development Center (AEDC), Air Force Systems Command (AFSC), USAF, was used to obtain the data presented. A description of the facility is contained in Ref. 2. Briefly, the tunnel consists of a d-c arc-heater, stilling chamber, conical nozzle of 15-deg half angle, test chamber with instrumentation, diffuser and pumping system.

Measurements of total enthalpy by calorimetery under the present conditions agree closely with total enthalpy computed on the basis of measured mass flow rate, total pressure, sonic throat area, and the assumption of thermodynamic equilibrium in the fluid upstream of the throat. However, since the computed relaxation lengths for molecular vibration downstream from the throat are from 10^2 to 10^4 times nozzle radius, all theoretical evidence indicates frozen flow from the throat onward. Thus, test-section flow characteristics are based on sudden freezing of the flow at the throat.

The operating conditions for this experiment were:

gas	= nitrogen
total pressure	= 1.21 atm (17.79 psia)
total temperature	= 3000 °K (5400°R)
total enthalpy	= 1560 Btu/lb

Depending on axial station in the nozzle:

Mach number	= 9.1 to 10.5
unit Reynolds number downstream of normal shock	= 40 to 80 per in.
mean free path downstream of normal shock	= 0.014 to 0.007 in.
diameter of uniform core	= 0.5 to 1 in.

3.0 MODEL AND DATA

The continuous mode of operation of the LDH Tunnel made it possible to utilize the relative simplicity of a steady-state measurement for heat transfer. The basic probes used are shown in Fig. 1. The heat transferred to the nose is conducted through the shaft to the heat sink which consists of a water jacket maintained at 55° to 65°F. The shaft is of known thermal properties and dimensions, and only a temperature distribution along the shaft need be measured to determine the heat flux along the shaft. The nose-shaft combination is insulated from the body of the probe so that heat flux from the nose travels only through the shaft. For this insulation, both an insulating material and physical isolation were tried, with approximately equal results for the same model configuration. In another instance, the physical separation or "air gap" proved superior.

TABLE 1

TABULATED VALUES OF MEASURED HEAT TRANSFER TO HEMISPHERICAL NOSE

1/4-in.-diam Hemispherical Nose $\dot{q}_{average}$, Btu/sq ft-sec				1/2-in.-diam Hemispherical Nose $\dot{q}_{average}$, Btu/sq ft-sec			
Re_2	min	max	avg	Re_2	min	max	avg
4.97	6.50	7.95	7.26	10.0	5.80	6.83	6.42
5.13	7.25	8.14	7.59	10.3	6.40	6.98	6.67
5.31	7.32	7.90	7.59	10.6	6.65	7.19	6.87
5.49	7.60	7.90	7.75	11.0	6.96	7.42	7.15
5.74	7.93	8.34	8.11	11.5	7.07	7.60	7.29
6.06	8.27	8.96	8.45	12.1	7.19	7.72	7.51
6.36	8.61	8.78	8.68	12.7	7.51	7.92	7.76
6.67	8.95	9.00	8.97	13.3	7.68	8.15	7.92
7.14	8.95	9.36	9.20	14.3	7.96	8.47	8.21
				15.4	8.28	8.69	8.44
				16.8	8.63	9.07	8.87
				18.3	8.93	9.64	9.31
				19.9	9.54	10.15	9.85

TABLE 2

TABULATED VALUES OF MEASURED HEAT TRANSFER TO FLAT-FACED NOSE

1/4-in.-diam Flat-Faced Probe $\dot{q}_{average}$, Btu/sq ft-sec				1/2-in.-diam Flat-Faced Probe $\dot{q}_{average}$, Btu/sq ft-sec			
Re_2	min	max	avg	Re_2	min	max	avg
4.97	16.7	19.5	18.1	10	10.9	13.2	12.0
5.13	20.1	20.2	20.2	10.3	11.5	13.3	12.4
5.31	20.1	20.9	20.4	10.6	12.1	13.9	13.2
5.49	20.6	21.1	20.9	11.0	12.7	14.1	13.4
5.74	21.1	21.4	21.3	11.5	12.9	14.8	14.1
6.06	21.5	21.7	21.6	12.1	13.3	14.9	14.1
6.36	21.4	22.9	22.1	12.7	14.5	16.0	15.4
6.67	20.7	23.9	22.7	13.3	15.2	16.2	15.7
7.14	21.4	21.4	21.4	14.3	16.1	16.9	16.5
				15.4	16.9	17.5	17.2
				16.8	17.9	18.6	18.2
				18.3	18.9	19.3	19.1
				19.9	20.3	20.3	20.3

The probe noses were smooth copper and were not highly polished. Nose temperature was maintained at approximately 300°F during tests.

Possible error in the measurement of heat flux includes:

1. error in measurement of heat flux along shaft considering errors in thermal conductivity of copper, cross sectional area, temperature read-out = 1.8 percent
2. error due to heat exchange in the probe, including thermocouple wires (assuming temperatures in probe shell are the same as in central stem, and gradient in thermocouple wire is equal to that in central stem) = 3.7 percent
3. error due to radiative loss from nose = 1 percent
4. total estimated error considering all effects additive = 6.5 percent.

The above is not necessarily the maximum error that could exist. However, it does assume all errors additive, which is not necessarily true.

4.0 BASIS FOR COMPARISON OF DATA AND THEORIES

The quantity obtained directly from the measurements was the total heat flux to the nose. This was divided by the wetted area of the nose to give the average flux per unit area. This section is devoted to a discussion of the adjustments necessary to compare these data qualitatively with results of work by others.

A problem arose in the comparison of the measured average* values with theories presented for stagnation-point heat transfer because the theoretical distribution appropriate to the flow conditions is not available in all cases. This left no recourse except the arbitrary assumption that one of the theories for thin boundary-layer flow (higher density) may be used to obtain the relation between average and stagnation-point heating rates at very low Reynolds numbers. This was done by assuming that Lees' distribution (Ref. 3) was valid for the case of the hemispheres. For the case of the flat-nosed models, the distribution computed by Vinokur (Ref. 4) was used. While these assumptions regarding distribution lack

*Average, as used herein, refers to the heat-transfer rate applied to the entire nose which consisted of either a hemisphere or circular disk.

justification, the error incurred probably is acceptable for qualitative comparisons with theory. The stagnation-point values inferred from these distributions are as follows:

Nose Shape	Distribution	$\dot{q}_o$	$\dot{q}_{o\,fm} = \rho_\infty U_\infty^3/2$
Hemisphere	(Ref. 3)	$2.50\ \dot{q}_{avg}$	$2.00\ \dot{q}_{avg\,fm}$
Flat Face	(Ref. 4)	$0.756\ \dot{q}_{avg}$	$\dot{q}_{avg\,fm}$

Lees' theory (Ref. 3) was used to calculate the stagnation-point heat-transfer rate for the thin boundary-layer regime, using the formula

$$\dot{q}_o = 0.5\sqrt{2}\,Pr^{-0.67}\left[\rho_2\mu_2\,(dU_e/ds)_o\right]^{0.5}(H_o - H_w) \quad (1)$$

with $Pr = 0.71$ and dU_e/ds based on experimental data for both nose shapes from Refs. 5 and 6. A form of Eq. (1) used later because of its convenience is

$$\dot{q}_o\sqrt{Re_2}/(\rho_\infty U_\infty^3/2) = \frac{0.707}{Pr^{0.67}}\sqrt{\frac{\rho_2}{\rho_\infty}}\sqrt{\frac{R}{U_\infty}\left(\frac{dU_e}{ds}\right)_o}\,\frac{2H_o\,(1 - H_w/H_o)}{U_\infty^2} \quad (2)$$

The distribution by Vinokur (Ref. 4) was obtained from the theory of Kemp, Rose, and Detra (Ref. 7) using, in place of a Newtonian theory for inviscid flow, the constant-density solution by Vinokur (Ref. 8).

One of the most recent theories available for predicting heat-transfer rates in the vicinity of the stagnation region of a hemispherical body in the flow regimes investigated is that of Cheng (Ref. 9). This theory is based on the continuum, thin shock-layer approximation with constant specific heats and a linear temperature-viscosity relation. The governing differential equations are simplified to a consistent order of magnitude by omitting terms which belong to an order of $\epsilon = (\gamma - 1)/2\gamma$ higher than the terms retained. The resulting equations are then solved to fit the appropriate set of boundary conditions which are also approximated to the same degree as the equations. The most restrictive assumptions concern the constant specific heats and the linear temperature - viscosity relation insofar as the gas model is concerned.

An unresolved point is the appropriateness of the thin shock-layer assumption. Cheng requires $\lambda_2/(R\sqrt{\epsilon}) \ll 1$, yet in the present experiments this quantity was as high as 0.3. He also requires $\lambda/R \ll 1$, and

using the results of Ref. 9 one finds $\Delta/R \approx \epsilon/2 \approx 0.08$. Shock thickness is neglected, and from Ref. 9 it is estimated that the shock thickness in the experiments was as much as one-fourth nose radius, i.e.,

$$d/R = \lambda_2 \sqrt{\epsilon}/(1 - 2\sqrt{\epsilon})R \approx 0.28 \qquad (3)$$

Van Dyke (Ref. 10) has pointed out that the model consisting of a nearly all viscous shock layer with a negligibly thin shock wave is not realistic.

Some of the theories presented are for a limiting cold wall, i.e., $H_w/H_o \approx 0$. Therefore, results of these theories are multiplied by $(H_o - H_w)/H_o$ where necessary since $H_w/H_o = 0.123$ in the present experiments. This factor, plus the distribution factor already given, results in Cheng's theoretical result being multiplied by 0.88 (0.4) = 0.352 to give a theoretical average heat-transfer rate to the entire nose surface for comparison with the measured average values on the hemisphere.

Levinsky and Yoshihara (Ref. 11) also have presented an analysis of heat transfer in low-density flow. Their calculations were based on $Pr = 3/4$ and $\gamma = 5/3$, so an appropriate adjustment to the absolute value of heat-transfer rate would have to be made on the basis that

$$\dot{q}_{avg} \sqrt{Re_2}/(\rho_\infty U_\infty^3/2) \propto Pr^{-0.67} \left[(\gamma - 1)/\gamma\right]^{0.25} (\rho_2/\rho_\infty)^{0.5} \qquad (4)$$

as derived from Eq. (1) using the velocity gradient given for Newtonian flow. For $M_\infty = 10$ and assuming equal velocities, enthalpies, and nose radii, Eq. (4) indicates that the curves for $\gamma = 1.667$ in Ref. 11 should be raised 16 percent for $\gamma = 1.400$. However, this is not a factor in the presentation of these results on Fig. 2 because the nondimensional heat-transfer rate parameter, $\dot{q}_{avg} \sqrt{Re_2}/\dot{q}_{avg\ fm}$ is normalized to the theoretical level of the present data as computed by Lees' method for the present test conditions. The same method of normalization has been used in presenting the results from Ref. 12 on Fig. 2 of this report.

The experimental data published by Wittliff and Wilson (Ref. 13) are compared with the new data. The data published in Ref. 13 were obtained at nearly equal Mach numbers but lower enthalpies in comparison to the present data. However, the nozzle flow of the shock tunnel experiments presumably was not frozen as it was in the LDH Tunnel.

Thus on Fig. 2, it is to be noted that the curves and data representing Refs. 11, 12, and 13 correspond to different density ratios and specific heat ratios than the experimental data from the LDH Tunnel. Since these fluid characteristics would affect the magnitude of secondary effects, the comparison is not direct in these cases. It is most nearly direct for the

theory of Ref. 9 and the data of Ref. 13. It is well to note that it also had been assumed that the second-order effects are independent of the absolute magnitude of the heat-transfer rate at high Reynolds numbers. This is believed to be allowable in the cases compared herein.

Notwithstanding the efforts to put the results from theories and experiments on a footing which would allow approximate quantitative comparison, it must be emphasized once again that the present data refer to average heat-transfer rates to an entire nose, which means that the effects of vorticity, etc., are integrated over that area. On the contrary, the most directly comparable theories and other data apply to the stagnation point, and the integrated or average effect of the secondary factors is not known. The comparison presented for the hemispherical nose has been made possible by using the relation between average and stagnation point rates given by Lees' theory for high Reynolds numbers where the second order factors exert no influence.

Chung (Ref. 14) and others have called attention to the effect produced on heat-transfer rates when nonequilibrium flow exists in the viscous shock layer at the stagnation region. In the present case, molecular vibration represents the major mode of possible nonequilibrium in this region since there is negligible dissociation of nitrogen at 3000 °K. Vibrational nonequilibrium normally is neglected in this context because it can, at most, account for relatively small percentage changes in comparison with other factors. However, it is worthwhile to consider the subject briefly.

In the present experiments, shock wave and boundary-layer thickness estimated separately by the usual methods (c.f. Ref. 10) are of the order of 0.1 in. Thus, it is conservative in regard to relaxation to consider shock-layer thickness, $\Delta \approx 0(R)$. If this distance and the velocity immediately behind the shock, U_2, are taken as characteristic of the region in question, a transit time for molecules of the order of 10^{-5} sec is derived. From Blackman (Ref. 15) at the temperature and pressure behind the shock in the present experiments, it is found that the relaxation time for nitrogen vibration is approximately 10^{-2} sec. In view of these estimates, it is not unreasonable to assume that frozen flow existed in the shock layer around the noses of the test bodies. Thus, in calculating the theoretical heat-transfer rates for comparison with the measurements, it is assumed that the normal shock occurs in a fluid with vibration frozen, but it is further assumed that the energy concentrated in molecular vibration is transmitted to the nose.* The difference between heat-transfer

*This assumption may be questioned. If the frozen enthalpy is not assumed recovered, agreement of the present data and the theories of Refs. 9, 11, and 12 would be improved in the case of the hemisphere. No comparison is possible for the flat face.

rate with the chosen flow model and an assumed equilibrium normal-shock process is small, i. e., about one percent in the present case.

5.0 RESULTS AND CONCLUSIONS

The considerations relative to comparison of the new measurements with various published theories and data are outlined in the previous section. The salient point is that the comparisons must remain qualitative to some degree because the theories and other data concern the stagnation point rather than the entire nose.

Figures 2 and 3 present the results. Only the theories of Cheng, Levinsky and Yoshihara, Probstein and Kemp, and the data of Whittliff and Wilson are presented for comparison. A description of effects on heat-transfer rate at low Reynolds numbers with dissociation is given in Ref. 16* where second-order effects are estimated to be larger than for a nondissociating gas when both gases attain thermo-chemical equilibrium behind the bow shock.

Behavior of the data appears qualitatively in agreement with results of the most appropriate theories and previous experiments. The hemisphere clearly displays the anticipated fall of heat transfer relative to the level at high Reynolds numbers. The Reynolds numbers where this occurs also are as expected. There is an indication that the data at the lowest values of Re_2 on Fig. 2 depart from the extrapolated, theoretically derived curves. First, it should be noted that the data extend to lower Reynolds numbers than are compatible with the flow models assumed for theoretical analysis. Second, the earlier remarks on the relation of average rates as opposed to stagnation-point rates may be relevant. Intuitively it seems that the combined effects of vorticity, slip, temperature jump, and displacement thickness would produce an integrated or average effect somewhat different from the effect at the stagnation point.

The flat-faced body represented in Fig. 3 seemingly exhibits an influence of second-order effects comparable to the hemisphere when the latter is in a range of Reynolds numbers where heat-transfer rate is

---

*An error seems evident in Ref. 16 in regard to the curve representing Levinsky's and Yoshihara's calculation. In the opinion of the present authors that particular curve should be shifted to the left on the Reynolds number scale by a factor of μ_∞/μ_2 in Fig. 7 of Ref. 16. It is suspected that this is the order of magnitude discrepancy mentioned therein.

elevated relative to the thin boundary-layer value due to dominance of the vorticity effect. The constant-density, subsonic flow field on which the heating rate distribution of Ref. 4 is based cannot be valid at Reynolds numbers where a fully merged shock layer exists for a highly cooled body. Thus, some of the difference between theory and experiment seen in Fig. 3 would be expected for this reason. There are no theoretical or other experimental comparisons to be drawn, but data applying to the flat nose appear credible in light of results for the hemisphere and of consideration of the difference in their flow fields.

Theoretical analyses of the heat-transfer rates are believed valid only part way into the flow regimes represented in these experiments. Analyses based on flow models corresponding to Reynolds numbers somewhat in excess of the highest range covered here have yielded results differing by several hundred percent (Ref. 16). In such a situation, the availability of additional experimental data is most desirable.

REFERENCES

1. Probstein, R. F. "Shock Wave and Flow Field Development in Hypersonic Re-Entry." American Rocket Society Journal, Vol. 31, No. 2, February 1961, pp. 185-194.
2. Potter, J. L., Kinslow, M., Arney, G. D., Jr., and Bailey, A. B. "Description and Preliminary Calibration of a Low-Density, Hypervelocity Wind Tunnel." AEDC-TN-61-83, August 1961.
3. Lees, L. "Laminar Heat Transfer Over Blunt-Nosed Bodies at Hypersonic Flight Speeds." Jet Propulsion, Vol. 26, No. 4, April 1956, p. 259-69, 274.
4. Vinokur, M. "Laminar Heat-Transfer Distribution on Oblate Ellipsoidal Noses in Hypersonic Flow." Journal of the Aerospace Sciences, Vol. 29, No. 1, January 1962, pp. 113-114.
5. Boison, J. Christopher. "Experimental Investigation of the Hemisphere-Cylinder at Hypervelocities in Air." AEDC-TR-58-20, October 1958.
6. Chones, A. J. "Heat Transfer and Pressure Measurements on Flat-Faced Flared-Tail Circular Cylinders and Normal Disks." NAVORD Report 6669, June 1959.
7. Kemp, N. H., Rose, P. H., and Detra, R. W. "Laminar Heat Transfer around Bodies in Dissociated Air." Journal of the Aero Space Sciences, Vol. 26, No. 7, pp. 421-430, July 1959.

8. Vinokur, M. "Inviscid Hypersonic Flow Around Blunt Bodies." Lockheed Missiles and Space Division, LMSD-48454, March 1959.

9. Cheng, H. K. "Hypersonic Shock-Layer Theory of the Stagnation Region at Low Reynolds Number." Cornell Aeronautical Laboratory Report No. AF-1285-A-7, April 1961.

10. Van Dyke, M. "Second-Order Compressible Boundary-Layer Theory with Application to Blunt Bodies in Hypersonic Flow." AFOSR-TN-61-1270, July 1961.

11. Levinsky, E. S. and Yoshihara, Hideo. "Rarefied Hypersonic Flow Over a Sphere." Hypersonic Flow Research, Vol. 7 of ARS Series on Progress in Astronautics and Rocketry, Academic Press, New York, 1962, pp. 81-106.

12. Probstein, Ronald F. and Kemp, Nelson H. "Viscous Aerodynamic Characteristics in Hypersonic Rarefied Gas Flow." Journal of the Aerospace Sciences, Vol. 27, No. 3, March 1960, pp. 174-192, 219.

13. Wittliff, Charles E. and Wilson, M. R. "Low Density Stagnation-Point Heat Transfer in Hypersonic Air Flow." Cornell Aeronautical Laboratory ARL Technical Report 60-333, December 1960.

14. Chung, P. M. "Hypersonic Viscous Shock Layer of Nonequilibrium Dissociating Gas." NASA TR R-109, 1961.

15. Blackman, V. "Vibrational Relaxation in Oxygen and Nitrogen." Journal of Fluid Mechanics, Vol. 1, P. 1, pp. 61-85, May 1956.

16. Goldberg, L. and Scala, S. "Mass Transfer in the Hypersonic Low Reynolds Number Viscous Layer." IAS Preprint No. 62-80, Presented at the IAS 30th Annual Meeting, New York, N. Y., January 22-24, 1962.

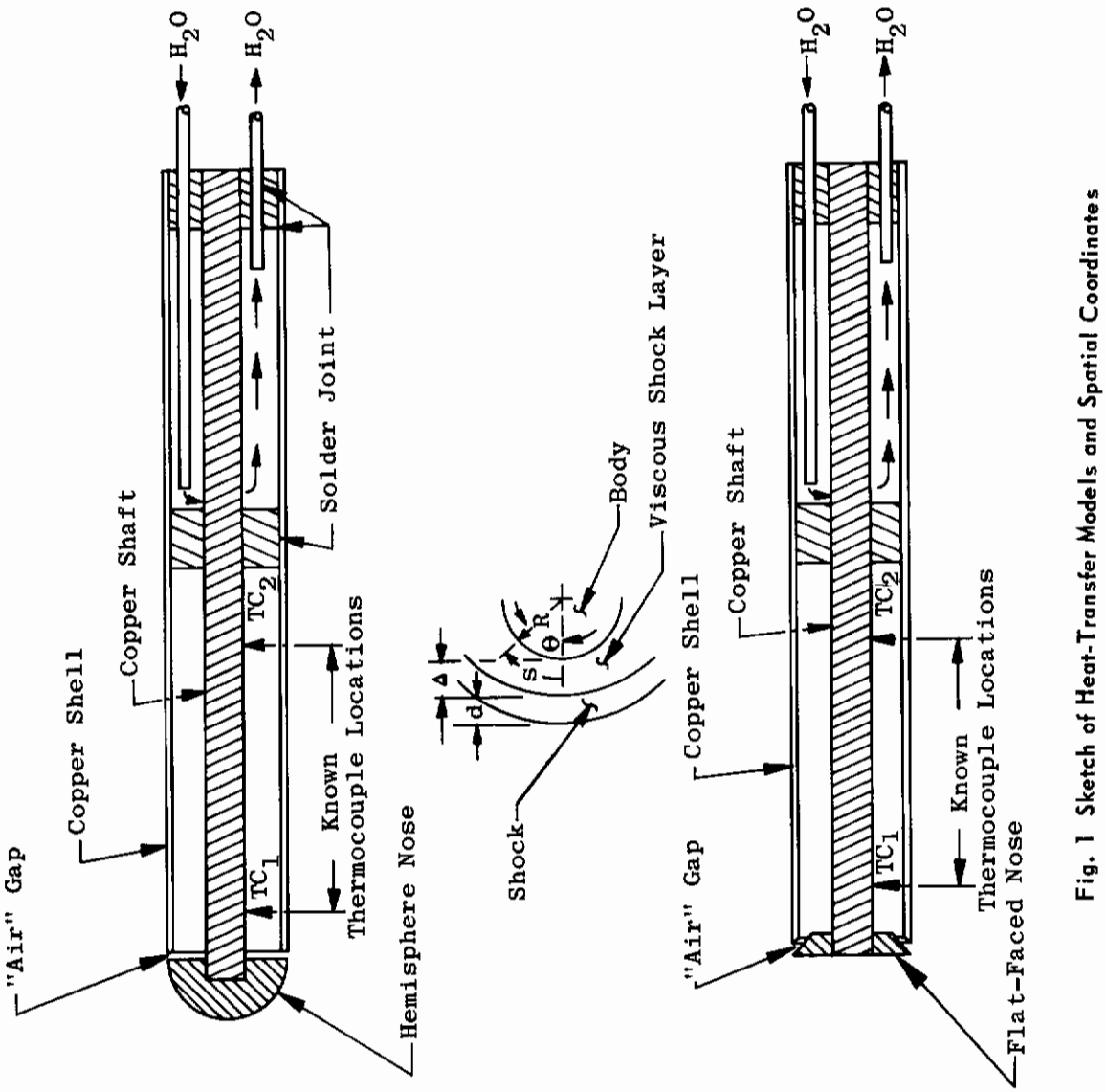

Fig. 1 Sketch of Heat-Transfer Models and Spatial Coordinates

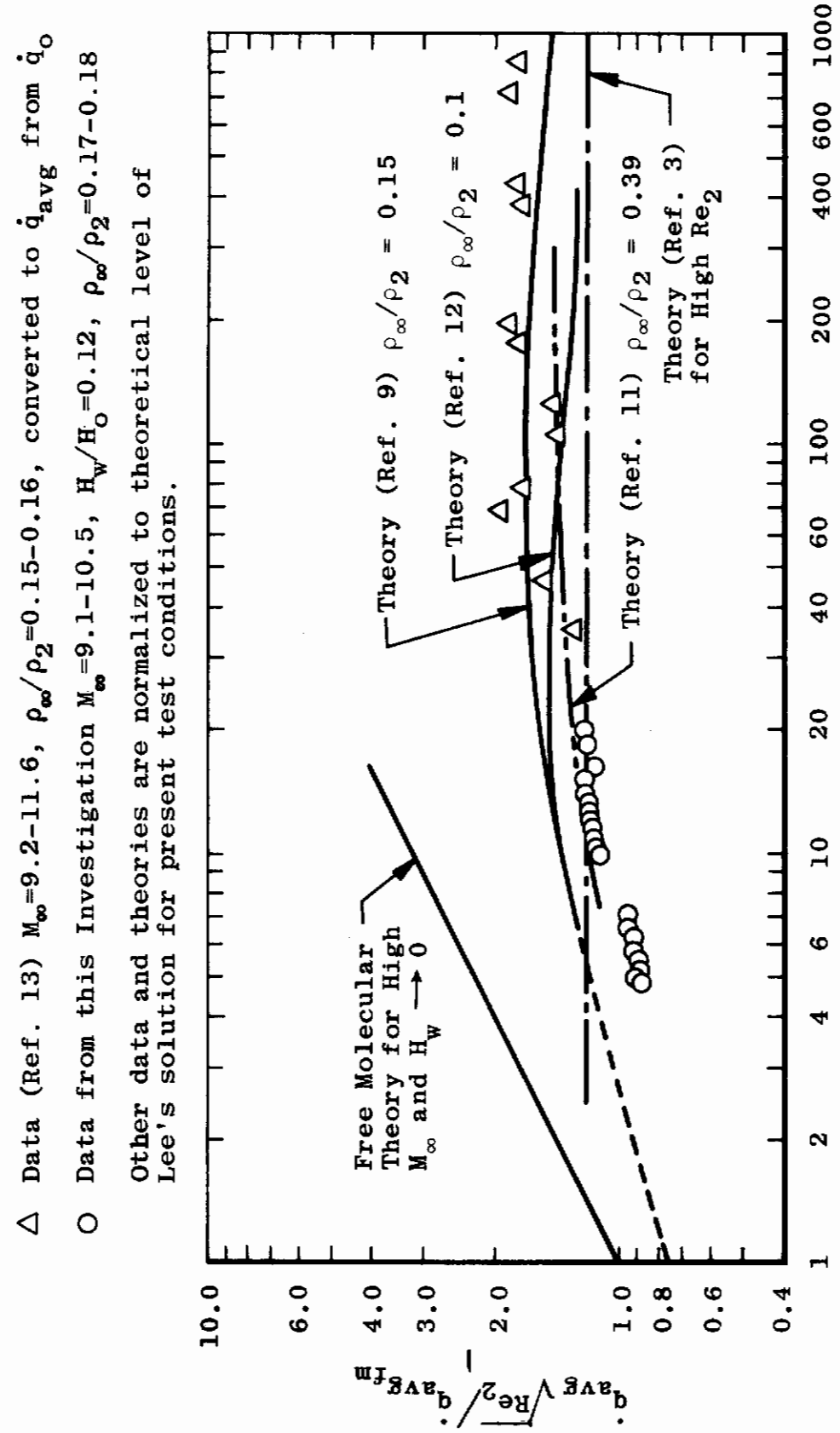

Fig. 2 Heat-Transfer Rate to a Hemispherical Nose; Comparison of Data and Theory

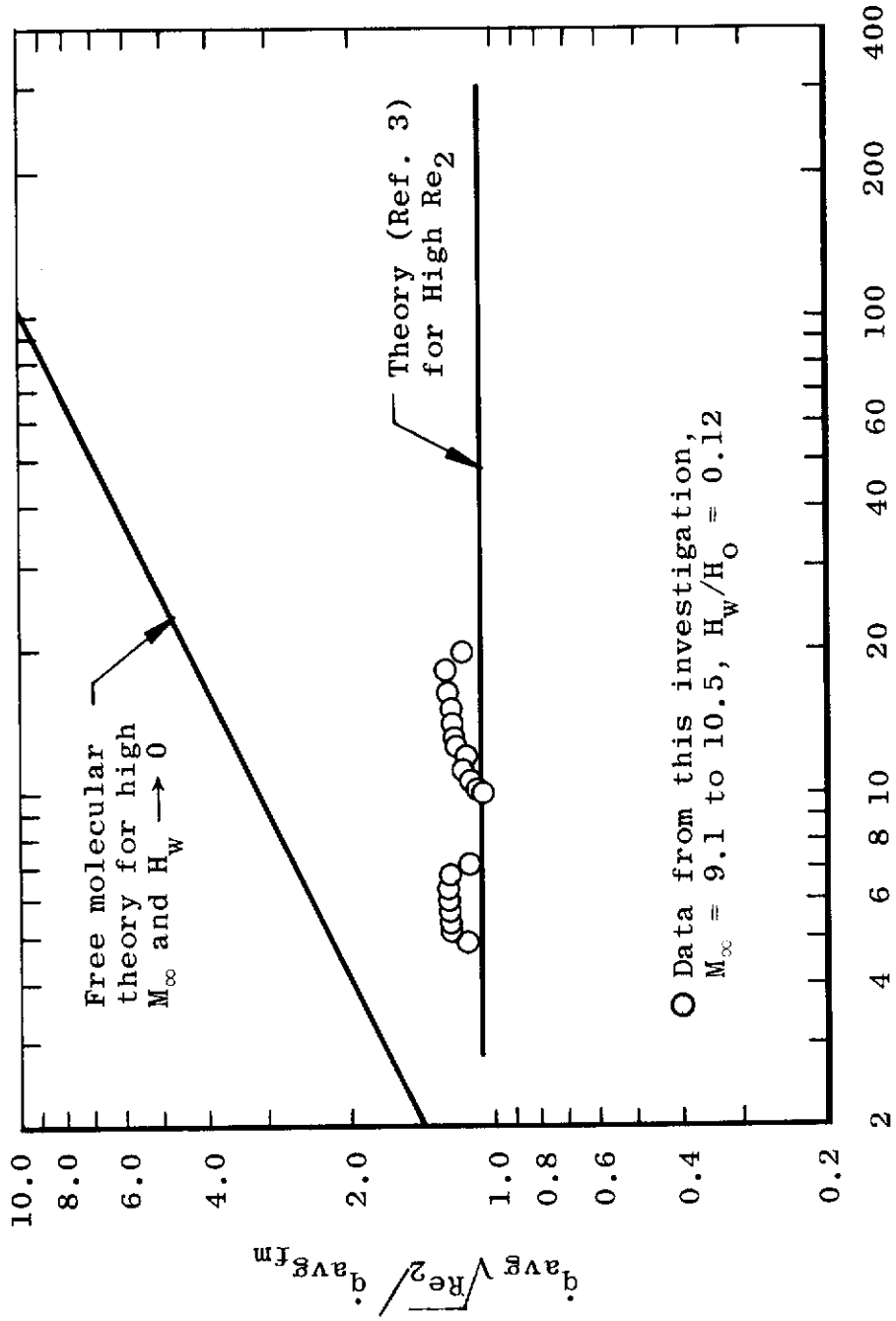

Fig. 3 Heat-Transfer Rate to a Flat Nose